Mixed mantle provenance: diverse garnet compositions in polymict peridotites, Kaapvaal craton, South Africa

H.-F. Zhang [a,b,*], M.A. Menzies [b], D. Mattey [b]

[a] *Laboratory of Lithosphere Tectonic Evolution, Institute of Geology and Geophysics, Chinese Academy of Sciences, P.O. Box 9825, Beijing 100029, P.R. China*
[b] *Department of Geology, Royal Holloway University of London, Egham, Surrey TW20 0EX, UK*

Abstract

Garnet compositions are used to understand mantle petrogenesis and to reconstruct the lithostratigraphy of the shallow mantle (< 200 km). However, garnets in polymict peridotites from the Kaapvaal craton (> 2500 Ma) have a centimeter-scale elemental and stable isotopic variability suggestive of a mixed mantle provenance. The chemical heterogeneity of the garnets is similar to that reported from rocks sampled over a considerable depth and temperature range within the lower lithosphere. For example garnets found in polymict peridotites are similar to garnets found in sheared and granular peridotites, 'cold' and 'hot' lherzolites, peridotitic (P-type) diamond inclusions, and garnets from polybaric (50–200 km) peridotites (i.e. spinel, garnet and diamond facies). These data indicate that the Kaapvaal cratonic root has been disturbed by complex processes possibly associated with crack propagation and entrainment that juxtaposed garnet-bearing lithologies of diverse petrogenesis, provenance and depth. This has preserved chemical disequilibrium in the high pressure minerals in what is, in effect, a mantle breccia possibly associated with kimberlite precursors.
© 2003 Elsevier B.V. All rights reserved.

Keywords: Kaapvaal craton; polymict peridotite; garnet; mantle provenance

1. Introduction

Garnet is an important constituent in the Earth's upper mantle at depths > 80 km (ca. 2.5 GPa). It occurs in rocks like eclogite, peridotite and pyroxenite, as megacrysts or discrete xenoliths, and as solid inclusions in diamonds. Its resistance to alteration accounts for its predominance in mineral concentrates and its value as a petrogenetic indicator mineral especially during diamond exploration. Overall garnets from the mantle display heterogeneities in major elements, in particular Cr_2O_3 and CaO, rare earth elements (REE), high field strength elements (HFSE; Ti, Zr, Y, Ga), and isotopes (Sr, Nd, O, Os, Hf). The composition of garnet concentrates from volcanic rocks is widely used to understand the nature of the mantle protolith, to reconstruct the lithostratigraphy of cratonic and circum-cratonic shallow mantle and to understand diamond petrogenesis [1–11].

* Corresponding author. Tel.: +86-10-62007821;
Fax: +86-10-62010846.
E-mail address: hfzhang@mail.igcas.ac.cn (H.-F. Zhang).

The main objective of this study is to investigate the mineralogical and geochemical variability in a unique suite of mantle rocks which are believed to have experienced a complex process of melt migration and concomitant deformation. In this paper the aims are to better understand aspects of their formation through the study of the garnets. In particular:

1. Paragenesis – To ascertain the compositional affinity (and thus the probable provenance) of the garnets – peridotite (low Ca harzburgite, lherzolite), eclogite or megacryst suites.
2. Lithostratigraphy – To evaluate the implications of the polymict rocks for keel lithostratigraphy and whether garnet composition is uniquely associated with particular rock types.
3. Deformation – To establish the extent to which deformation has affected garnet chemistry.
4. Equilibrium – To investigate the trace element and isotopic equilibrium between the garnets and other juxtaposed minerals (e.g. olivine-orthopyroxene-clinopyroxene-ilmenite).
5. Melt processes – To consider the composition of hypothetical melts in equilibrium with the garnets.

2. Petrography and mineralogy

Four polymict xenoliths from Kimberley are used in this study (i.e. JJG1414, BD2394, BD344 and BD2666) [12]. Polymict xenoliths are clinopyroxene-poor (0–3%) 'harzburgites' comprising olivine, orthopyroxene, clinopyroxene, garnet, phlogopite, ilmenite and rutile. Polymict peridotite, JJG1414 (Fig. 1A), is strongly deformed and contains porphyroclastic olivine, enstatite, diopside, garnet, and ilmenite set in a dark green neoblastic olivine matrix. Phlogopite was not found in this xenolith. Other polymict peridotites
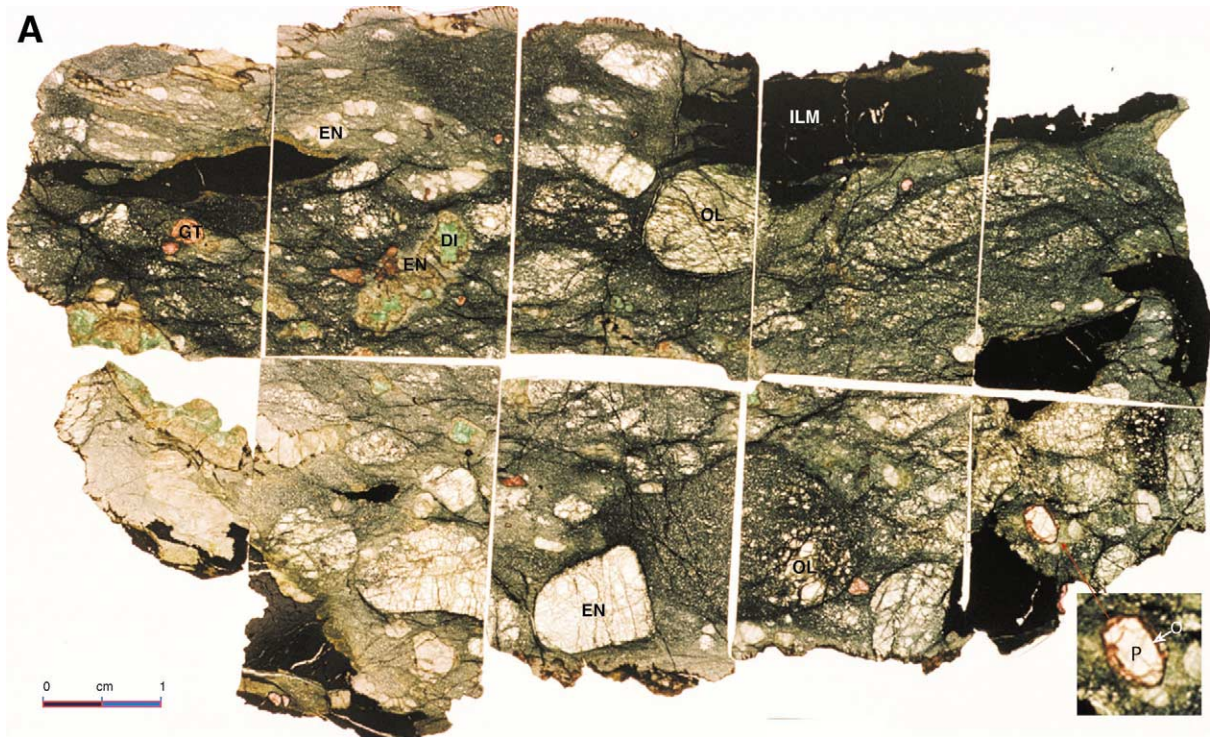

Fig. 1. Photograph of double-polished polymict xenolith. (A) JJG1414. (B) BD2394. Enlarged areas in JJG1414 and in BD2394 show an apparent garnet zonation in color with the pink core (P) and the orange rim (O) and the replacement between minerals. OL, EN, DI, GT, ILM, and PHL represent olivine, enstatite, diopside, garnet, ilmenite, and phlogopite, respectively.

(BD2394, BD344 and BD2666) are less deformed and are composed of granular olivine and enstatite with minor granular garnet, diopside, ilmenite, and phlogopite set in an intergranular fine-grained matrix of olivine, secondary phlogopite and ilmenite (Fig. 1B). All the coarse diopsides in the polymict rocks have brown enstatite rims, partially or completely replacing the host diopside [13]. Replacement is usually accompanied by the formation of finely disseminated oxides. The grain boundaries between the diopside and the enstatite rims are poorly defined and the rim enstatites are sheared. The texture relationship of the diopside replaced by the enstatite and the systematic compositional variations between the coarse diopside and the rim enstatite are reported elsewhere [13]. This study provided evidence for the existence of harzburgites formed by silica- and calcium-rich metasomatism. Coarse diopside is also replaced by secondary phlogopite (Fig. 1B). The only secondary diopside found in BD2394 replaces enstatite (Fig. 1B). Phlogopites occur as large irregular dark brown phlogopite interstitial to other minerals (Fig. 1B), brown phlogopite and tiny euhedral phlogopite aggregates replacing garnet (Fig. 2b–d), olivine, enstatite, and diopside. Ilmenites from JJG1414 display a well-equilibrated, polygranular mosaic texture and 120° triple junctions are common, whilst ilmenites in BD2666 occur as irregular 'layers' [14]. Detailed descriptions of the mineralogy and geochemistry of the ilmenites in these polymict xenoliths are given elsewhere [14].

Garnets in these polymict xenoliths are minor but important constituents (Fig. 1A,B). There are

Garnet replaced by secondary phlogopite

Diopside replaced by secondary phlogopite

Enstatite replaced by secondary diopside

Enstatite replaced by secondary diopside

Fig. 1 (*Continued*).

a variety of colors within individual polymict xenoliths (Fig. 1A,B) and the garnets can be divided into two groups: light-colored (colorless-pink-or-ange) and dark-colored (brown-claret-lilac-purple). This distinction in color is matched by variations in major elements, trace elements and oxygen isotopes. For example, the light-colored garnets have lower Cr_2O_3 contents and higher oxygen isotopic ratios than the dark-colored garnets. The very presence of garnets, in one polymict peridotite, which displays a spectrum of colors encompassing almost all types of garnets from global kimberlite-borne mantle xenoliths, suggests a mixed provenance of garnet-facies mantle lithologies.

Garnets in JJG1414 occur as rounded discrete grains (Fig. 1A) or they co-exist with the rim enstatites. Grain sizes of the garnets are dominantly in the range of $0.5 \sim 4$ mm (Figs. 1A and 3a) with the lighter-colored garnets being generally larger than the darker-colored garnets. Pink garnets show a clear textural zonation (Fig. 1A), where the rims (orange) are usually darker than the cores (pink). Brown and claret-colored garnets, especially the euhedral ones, also have zoned textures (Fig. 2a), generally displaying a core, an internal and an external zone, and a water-bearing rim (Fig. 2a). This textural zonation corresponds to marked elemental and oxygen isotopic zonation with the rims being enriched in Ca, Ti, Cr, LREE, Sr and Nb, and depleted in Mg, Al and [18]O [15]. Such zoned garnets occur in peridotitic xenoliths from the Jagersfontein kimberlite pipe, South Africa, and have preserved chemical heterogeneities from complex mantle processes [11]. Garnets in other polymict xenoliths (BD2394, BD344, and BD2666) occur as rounded discrete grains (Fig. 1B). All the garnets in these
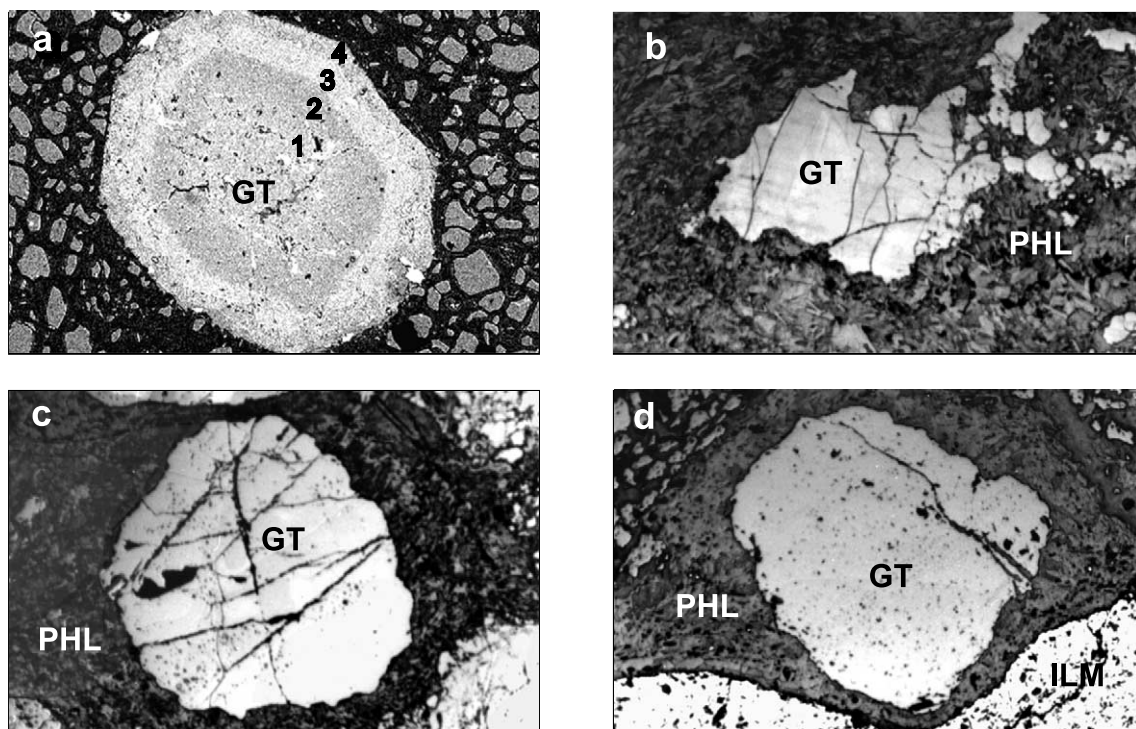

Fig. 2. The backscattered images. (a) A tiny euhedral zoned garnet in JJG1414. 1: the core, 2: the internal zone, 3: the external zone, 4: the water-, Na- and K-bearing rim. Garnet zonation is accompanied by compositional variation where CaO decreases and Cr_2O_3 and Al_2O_3 increase from the center to the external zone. (b) Lilac garnet replaced by tiny euhedral secondary phlogopite ± ilmenite in BD2394. (c,d) Lilac-purple garnet replaced by tiny phlogopite, ilmenite, and serpentine in BD2666. Width of the field is 1 mm in a, 2 mm in b–d.

polymict xenoliths have a dark rim (Fig. 1B) of secondary phlogopite ± ilmenite aggregates that clearly replace the garnets (Fig. 2b–d). Dark-colored garnets tend to be more susceptible to this replacement than the light-colored garnets. Such replacement of garnet by phlogopite does not occur in the polymict xenolith JJG1414. The lighter-colored garnets in BD2394, BD344, and BD2666 tend to be bigger in grain size than the darker-colored garnets (Figs. 1B and 3a), similar to JJG1414. Generally speaking, garnets in these polymict xenoliths have smaller grain sizes relative to other minerals such as olivine, enstatite, and diopside and are dominantly in the range of 0.2∼4 mm with one grain up to 7.6 mm (Fig. 3a). Major and trace elemental compositions and ratio of garnets are broadly co-related with grain sizes (Fig. 3b–d). Garnets with smaller grain sizes generally tend to have higher Ca and Nb contents and Ce/Yb ratios.
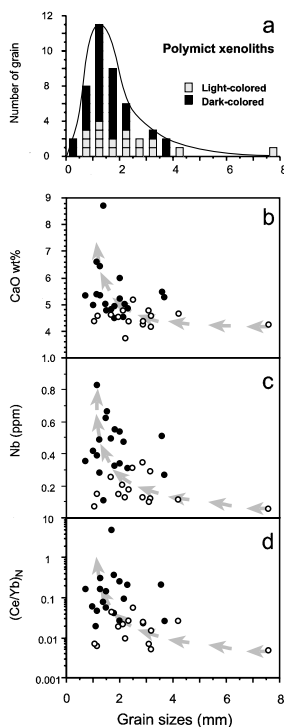
Fig. 3. (a) Histogram of garnet grains in polymict peridotites. (b–d) Compositional variations of Ca and Nb abundances and chondrite-normalized Ce/Yb ratios with garnet grain sizes. Open circles and filled circles represent light-colored and dark-colored garnets, respectively.

3. Analytical methods

Polymict peridotites were cut into normal thin-section slices that were doubly polished to ca. 500 μm thickness and photographed in detail (Fig. 1). The major and trace element abundances were respectively measured in situ on carbon-coated and gold-coated polished slices by electron microprobe (JEOL Superprobe) and ion microprobe (Cameca® ims-4f) at the Department of Geology, Birkbeck College, University of London and the Department of Geology and Geophysics, Edinburgh University, UK. Analyses with electron microprobe were performed with a beam of 15 keV and 15 nA focused to a spot ∼1 mm in diameter and analytical precision was estimated with 0.2 wt%. For trace element analysis with ion microprobe, the measurements were made with an 8 nA $^{16}O^-$ primary beam accelerated by 10 keV and focused to a spot of 15–20 μm in diameter. In order to obtain enough intensity, acquisition time was increased to 15 s per cycle for elements with extremely low concentrations (especially for LREE). The precision of the recorded count for most trace elements is within 10%. The coatings were then removed and the slices were mounted onto glass plates. Garnets were carefully removed under the binocular microscope and then cleaned with acetone in an ultrasonic bath for 20 min. Approximately 1.5 mg garnet was required for oxygen isotope analysis and the compositions were obtained using the laser fluorination technique at the Department of Geology, Royal Holloway, University of London, UK. The detailed measurement procedures and the precision for each method are available in [13,14,16,17].

4. Major and trace element geochemistry

Representative major and trace element concentration data for garnets in polymict peridotites are given in Table 1. Elemental abundances vary greatly between different samples, co-existing garnets in the same sample, and within individual garnets. The variation in Cr_2O_3 and CaO in pyropic garnets (Fig. 4a,b) is considerable and straddles the compositional 'fields' previously defined

Table 1
Representative analyses of major and trace element concentrations and oxygen isotopic ratios in Kimberley polymict garnets

Garnet	BD344		BD2394													
Color	Claret	Purple	Y. Pink	Y. Pink	Y. Pink	Y. Pink	Pink	Pink	Pink	Pink	Orange	Colorless	Claret	Lilac	Lilac	Purple
	Fig. 5c	Fig. 5c	Fig. 5a	Fig. 5a	Fig. 5a	Fig. 5a	Fig. 5a	Fig. 5a	Fig. 5a	Fig. 5a	Fig. 5b	Fig. 5c	Fig. 5b	Fig. 5b	Fig. 5d	Fig. 5c
Major element compositions (%)																
SiO_2	42.86	42.11	43.07	42.77	42.33	42.65	42.66	42.54	42.42	43.01	42.47	42.17	42.59	42.71	43.33	41.90
TiO_2	0.24	0.40	0.17	0.54	0.51	0.30	0.36	0.69	0.67	0.32	0.26	0.43	0.45	0.60	0.00	0.49
Al_2O_3	19.72	18.92	23.07	21.80	22.27	23.00	22.49	19.63	21.89	22.79	21.00	22.85	19.37	20.51	20.81	18.02
Cr_2O_3	5.61	6.30	0.36	1.30	0.71	0.26	1.27	4.54	1.34	0.66	2.72	0.00	5.14	3.50	4.25	6.44
FeO	6.11	5.79	10.56	9.56	9.95	11.35	8.59	8.56	10.35	7.97	9.13	11.61	6.70	6.97	6.30	7.88
MnO	0.29	0.39	0.44	0.33	0.35	0.31	0.35	0.44	0.42	0.28	0.48	0.34	0.45	0.27	0.35	0.34
MgO	20.90	20.54	18.65	19.22	18.87	18.42	19.60	19.27	18.77	20.02	18.69	14.56	20.12	19.97	20.12	18.45
CaO	4.88	5.41	4.39	4.60	4.36	3.72	4.66	4.59	4.18	4.25	4.78	8.70	5.01	5.26	5.34	5.98
	100.6	99.9	100.7	100.1	99.4	100.0	100.0	100.3	100.0	99.3	99.5	100.7	99.8	99.8	100.5	99.5
Mg#	0.86	0.86	0.76	0.78	0.77	0.74	0.80	0.80	0.76	0.82	0.78	0.69	0.84	0.84	0.85	0.81
Trace element concentrations (ppm)																
La	0.010	0.017	0.013	0.009	0.011	0.008	0.006	0.034	0.013	0.007	0.018	0.011	0.040	0.016	0.029	0.017
Ce	0.125	0.202	0.149	0.111	0.052	0.096	0.123	0.226	0.072	0.050	0.123	0.199	0.353	0.104	0.355	0.217
Pr	0.062	0.093	0.054	0.055	0.033	0.044	0.072	0.081	0.040	0.032	0.068	0.116	0.111	0.042	0.152	0.107
Nd	1.04	1.44	0.55	0.67	0.49	0.55	0.81	0.81	0.54	0.48	0.85	1.53	1.21	0.55	1.03	1.35
Sm	1.37	1.38	0.32	0.76	0.43	0.47	0.79	0.75	0.73	0.64	0.65	1.14	0.94	0.56	0.22	1.51
Eu	0.67	0.62	0.16	0.47	0.23	0.25	0.32	0.46	0.34	0.29	0.35	0.57	0.42	0.25	0.07	0.81
Gd	2.44	2.67	0.68	2.28	0.99	1.26	1.37	2.16	1.80	1.40	1.41	2.12	1.56	1.03	0.25	4.02
Tb	0.32	0.51	0.18	0.60	0.22	0.25	0.23	0.58	0.47	0.33	0.28	0.46	0.29	0.21	0.03	0.83
Dy	1.45	3.51	1.53	4.81	1.78	2.30	1.93	4.78	3.94	2.66	2.06	2.39	2.16	1.58	0.09	5.38
Ho	0.14	0.61	0.40	1.27	0.46	0.63	0.43	1.21	0.98	0.68	0.42	0.38	0.43	0.34	0.02	0.98
Er	0.22	1.44	1.33	4.29	1.64	2.19	1.23	3.75	3.42	2.24	1.54	0.96	1.45	1.07	0.19	2.71
Tm	0.03	0.17	0.20	0.67	0.28	0.37	0.18	0.57	0.57	0.43	0.22	0.12	0.23	0.16	0.04	0.35
Yb	0.16	1.15	1.49	4.79	1.95	2.65	1.28	3.92	3.84	2.90	1.49	0.64	1.67	1.07	0.30	2.24
Lu	0.03	0.16	0.24	0.74	0.31	0.46	0.17	0.58	0.55	0.52	0.27	0.13	0.26	0.18	0.07	0.31
Y	4.43	17.16	11.27	34.40	12.63	17.89	11.12	31.03	27.63	19.11	12.23	11.10	13.51	9.85	0.49	30.50
Sr	0.23	0.33	0.21	0.24	0.19	0.23	0.27	0.33	0.22	0.17	0.25	0.58	0.35	0.04	0.28	0.39
Zr	106	89.5	9.0	141	40.0	31.1	54.1	132	117	53.4	37.8	56.9	33.4	37.0	1.6	85.3
Hf	2.06	1.67	0.17	3.11	1.11	0.77	1.04	3.38	2.40	1.41	0.77	1.06	0.71	1.19	0.09	1.75
Nb	0.32	0.39	0.18	0.15	0.07	0.13	0.11	0.29	0.12	0.06	0.21	0.11	0.62	0.27	0.49	0.54
Oxygen isotopes (‰)																
$\delta^{18}O$	5.06	4.84	5.02	5.18	5.91	6.17	5.18	5.59	5.75	5.57	5.34	5.10	5.04	5.14	5.17	5.17

Table 1 (*Continued*).

Color	Pink core # Fig. 5a	Orange rim # Fig. 5b	Orange Fig. 5b	Brown Fig. 5b	Brown Fig. 5b	Brown Fig. 5c	Brown core[a] Fig. 5b	rim[a]	Claret Fig. 5c	Lilac Fig. 5c	Pink Fig. 5a	Pink Fig. 5a	Pink Fig. 5a	Brown Fig. 5c	Claret Fig. 5c	Lilac Fig. 5d	Purple Fig. 5c	Purple Fig. 5d
Major element compositions (%)																		
SiO_2	43.36	42.57	41.54	42.08	42.08	43.16	42.26	41.73	42.00	42.58	43.20	42.84	43.18	42.86	43.06	43.21	41.37	43.04
TiO_2	0.44	1.34	0.28	1.53	0.79	0.26	0.80	1.41	0.15	0.16	0.51	0.31	0.17	0.10	0.09	0.05	0.67	0.05
Al_2O_3	22.79	19.58	20.92	20.21	20.37	19.03	21.33	16.15	17.87	20.81	22.55	22.89	23.27	21.12	20.06	20.58	16.18	19.59
Cr_2O_3	0.79	4.01	2.50	2.63	3.13	6.46	2.22	4.10	7.29	3.58	1.17	0.59	0.43	3.71	5.05	4.42	8.58	5.61
FeO	7.26	7.52	11.37	7.06	7.12	5.52	7.15	4.67	7.24	6.66	8.14	9.55	9.54	6.79	6.07	6.00	7.80	6.08
MnO	0.19	0.31	0.39	0.28	0.33	0.33	0.22	0.23	0.34	0.26	0.33	0.52	0.33	0.50	0.31	0.23	0.44	0.13
MgO	21.13	20.29	17.53	20.96	20.37	21.29	20.45	16.07	19.00	20.21	19.78	18.74	19.34	19.7	20.45	20.76	17.93	20.59
CaO	4.24	4.39	5.19	4.53	4.94	4.48	4.82	9.44	5.48	4.79	4.55	4.78	4.61	5.22	4.98	5.37	6.61	4.83
	100.2	100.0	99.7	99.3	99.1	100.5	99.3	93.8	99.4	99.1	100.2	100.2	100.9	100.0	100.1	100.6	99.6	99.9
Mg#	0.84	0.83	0.73	0.84	0.84	0.87	0.84	0.86	0.82	0.84	0.81	0.78	0.78	0.84	0.86	0.86	0.80	0.86
Trace element concentrations (ppm)																		
La	0.017	0.031	0.032	0.351	0.126	0.183	0.036	0.904	0.095	0.018	0.036	0.011	0.022	0.046	0.013	0.013	0.027	0.132
Ce	0.175	0.321	0.370	1.270	0.536	0.702	0.493	1.810	0.623	0.329	0.242	0.093	0.198	0.723	0.264	0.186	0.280	1.970
Pr	0.056	0.127	0.206	0.240	0.166	0.287	0.182	0.218	0.231	0.165	0.079	0.048	0.074	0.326	0.144	0.141	0.129	0.853
Nd	0.63	1.60	2.21	2.21	1.80	3.60	2.23	1.52	3.06	2.24	0.76	0.87	0.58	4.29	1.90	4.27	1.50	5.13
Sm	0.43	1.34	1.31	1.63	1.41	2.29	1.88	1.16	2.65	3.04	0.58	0.77	0.30	3.85	1.54	2.36	1.46	0.34
Eu	0.20	0.61	0.46	0.89	0.68	0.97	0.99	0.64	1.01	1.49	0.28	0.39	0.14	1.89	0.59	0.40	0.78	0.06
Gd	0.90	2.77	1.27	4.01	3.14	2.99	4.07	3.26	3.21	6.58	1.40	1.60	0.56	6.46	1.60	0.71	3.82	0.07
Tb	0.19	0.65	0.27	0.86	0.71	0.42	0.96	0.79	0.51	1.17	0.35	0.33	0.11	0.84	0.18	0.07	0.88	0.01
Dy	1.76	4.78	1.73	6.74	5.69	2.01	7.15	5.71	2.64	6.18	3.11	2.98	1.06	3.60	0.91	0.18	6.98	0.06
Ho	0.49	1.05	0.41	1.43	1.21	0.31	1.50	1.44	0.38	0.73	0.81	0.69	0.26	0.47	0.18	0.04	1.44	0.01
Er	1.62	3.20	1.37	4.26	3.66	0.49	4.78	4.09	0.95	1.13	2.92	2.54	0.95	1.08	0.68	0.10	4.28	0.03
Tm	0.29	0.62	0.24	0.62	0.55	0.07	0.67	0.79	0.13	0.10	0.46	0.47	0.16	0.14	0.14	0.04	0.63	0.01
Yb	1.95	3.70	1.73	3.75	3.47	0.51	4.56	4.99	0.77	0.59	3.42	3.53	1.19	0.74	1.16	0.30	3.93	0.11
Lu	0.30	0.55	0.31	0.52	0.47	0.07	0.68	0.87	0.11	0.11	0.56	0.59	0.19	0.09	0.23	0.05	0.54	0.04
Y	13.63	31.76	11.60	39.19	32.74	8.87	39.92	36.75	10.93	20.20	24.10	20.08	7.73	12.54	6.58	0.98	42.10	0.21
Sr	0.27	0.47	0.39	1.28	1.12	1.88	0.64	82.60	0.57	0.34	0.37	0.17	0.16	0.51	0.61	0.24	0.57	0.95
Zr	23.1	148	43.8	152	200	126	208	138	138	300	40.5	55.7	10.6	61.7	41.2	18.0	119	2.9
Hf	0.66	3.11	0.99	3.68	4.50	2.39	4.23	4.33	2.37	4.72	1.20	1.33	0.35	0.78	0.82	0.56	3.11	0.02
Nb	0.13	0.35	0.31	0.47	0.33	0.56	0.45	0.56	0.51	0.67	0.15	0.10	0.26	0.34	0.42	0.35	0.83	0.50
Oxygen isotopes (‰)																		
$\delta^{18}O$	5.38	5.00	4.70	4.76	4.80	4.90	–	–	4.78	5.17	5.14	5.12	5.05	–	5.43	4.82	4.60	4.74

Mg# = Mg/(Mg+Fe) atomic ratio. Y. = yellowish. #: zoned garnet in Fig. 1A.
[a] Tiny euhedral zoned garnet in Fig. 2a where the rim contains water, potassium (0.5% K_2O), and sodium (4.65% Na_2O). Fig. 5a–d shows individual garnet grains plotted in the specified location of Fig. 5.
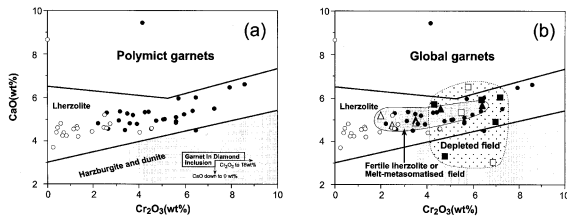
Fig. 4. (a) Centimeter-scale variation in Ca–Cr in garnets from polymict peridotites. Some rocks contain garnets with a range of Cr contents similar to sheared and granular lherzolites and discrete nodules [18]. Comparative fields for peridotites are taken from Sobolev et al. [20] and Meyer [21]. Note that none of the garnets from polymict peridotites have any affinity with low calcium harzburgites and dunites, despite their ubiquity in some cratonic keels. Open circles and filled circles represent light-colored and dark-colored garnets, respectively. (b) Comparison of garnets from polymict peridotites with garnets from the depleted, fertile, metasomatized peridotites [19]. Depleted field includes the garnets from the depleted (open square) and depleted/metasomatized peridotites (filled square). Fertile lherzolite or melt-metasomatized field represents the garnets from the fertile lherzolites (open triangle) and sheared lherzolites (filled triangle).

by garnets from sheared and granular lherzolites and garnets occurring as discrete nodules or megacrysts [6,18]. In other words, within the polymict peridotites there is a considerable heterogeneity in garnet composition that would normally be found in rocks of very diverse provenance derived from a considerable depth range within the lithospheric mantle (Fig. 4b). Even individual polymict peridotites have a wide range in Cr_2O_3 content. Dark-colored garnets have a high Cr, Ca content in relation to light-colored garnets which have a low Cr, Ca content. Interestingly, none of the pyropic garnets lie within the field defined by harzburgites and dunites (Fig. 4a), or the low calcium garnets found as solid inclusions in diamonds. All the garnets are from 'lherzolite' precursors and overlap with the field of fertile lherzolite, melt-metasomatized peridotites and depleted peridotites [19].

Chondrite-normalized REE profiles for pyropic garnets vary from strongly LREE-depleted to MREE-enriched or sinusoidal patterns (Fig. 5a–d). Chondrite-normalized LREE-depleted profiles occur in the light-colored (Cr-poor) garnets (Fig. 5a,b) and chondrite-normalized MREE-enriched

or sinusoidal REE patterns are observed in dark-colored (Cr-rich) garnets (Fig. 5c,d).

4.1. LREE-depleted patterns

All the light-colored garnets found in the polymict xenoliths have strongly LREE-depleted chondrite-normalized REE patterns (Fig. 5a). They are typically very low in the LREE $((La)_N < 0.1)$ and have a smooth chondrite-normalized abundance pattern. In contrast, the LREE-depleted patterns observed in orange-
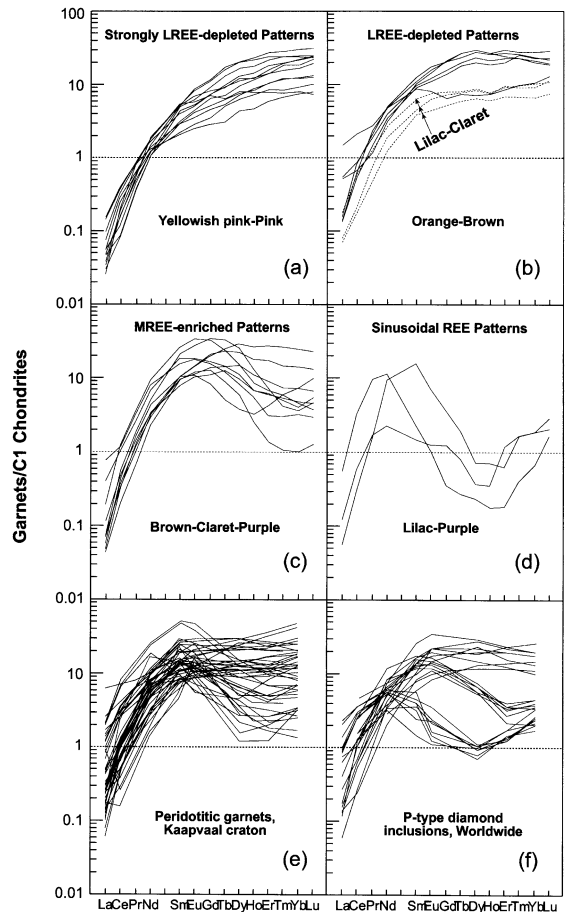
Fig. 5. Chondrite-normalized REE abundances in garnets from polymict peridotites. Note that garnets have a range of chondrite-normalized REE patterns similar to peridotitic garnets and P-type solid inclusions in diamonds. C1 chondrite values are from Anders and Grevesse [22]. Comparative data after Shimizu and Sobolev [23], Hoal et al. [24], Shimizu [25], and references therein.

brown garnets (Fig. 5b) have much higher LREE and variable MREE abundances ((La)$_N$ > 0.4). Some garnets have LREE-depleted patterns which differ from other LREE-depleted patterns in that they have a different MREE/HREE ratio (Fig. 5b).

4.2. MREE-enriched patterns and sinusoidal REE patterns

Garnets with MREE-enriched profiles occur in all the polymict peridotites (Fig. 5c). In some cases, the garnet is slightly enriched in Lu or Ho–Lu (Fig. 5c) and the REE profile has a sinusoidal shape. Sinusoidal REE profiles exist in three lilac-purple garnets (Fig. 5d) where the REE abundance varies dramatically. Additionally, a zoned garnet from JJG1414 (Table 1) has a much higher total REE abundance in the rim compared to the core.

Generally speaking, the chondrite-normalized
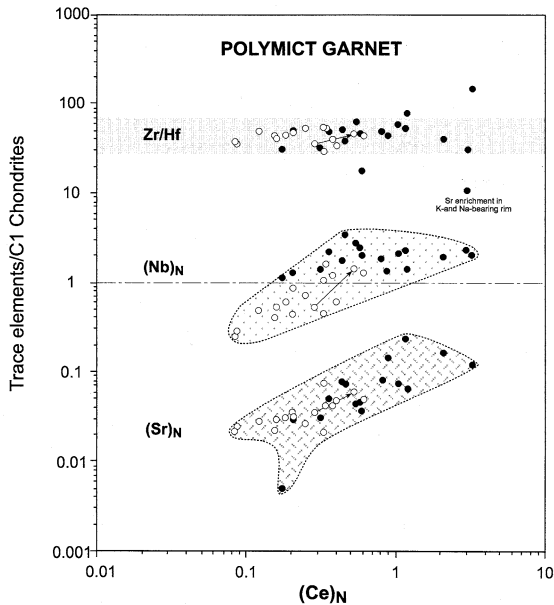
Fig. 6. LREE correlation with other trace element concentrations in garnets from the Kimberley polymict peridotites, South Africa. Note that whatever process accounts for the enrichment in the LREE also led to a systematic change in the concentration of Sr and Nb at near constant Zr/Hf ratio. Open circles and filled circles represent light-colored and dark-colored garnets, respectively.
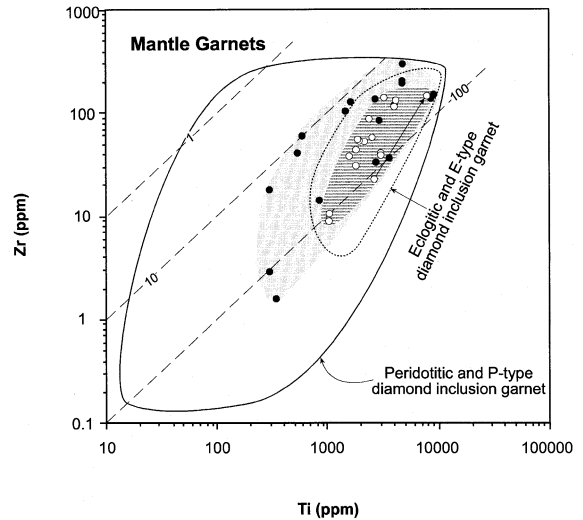
Fig. 7. Zr covariance with Ti in garnets from the Kimberley polymict peridotites. Ti was calculated from electron microprobe data. The garnets in polymict peridotites have a range in Ti/Zr that encompasses that observed in peridotitic and eclogitic parageneses and solid diamond inclusions (P- and E-type). Also shown are comparative fields for peridotites and P-type diamond inclusions [1,4,6,9,10,23,27–30], and from eclogites and E-type diamond inclusions [26,27,31–35]. Long dash lines are Ti/Zr isopleths. Open circles and filled circles represent light-colored and dark-colored garnets, respectively.

LREE-depleted profiles (Fig. 5a) are similar to those observed in peridotitic garnets and peridotite-type (P-type) diamond inclusions (Fig. 5e,f). However, the degree of LREE depletion in garnets from polymict peridotites is greater than that reported from peridotitic parageneses. The chondrite-normalized MREE-enriched and sinusoidal REE patterns are similar to those observed in solid garnet inclusions from P-type diamonds [10,23,26,27] and kimberlite-borne peridotites from South Africa [4,6,24].

With regard to other trace elements, garnets in polymict peridotites are extremely depleted in Sr (< 2 ppm). The Sr and Nb concentration in the garnets correlates positively with the LREE (Fig. 6). One K- and Na-bearing garnet rim is enriched in Sr (> 82 ppm) and, in general, the dark-colored (Cr-rich) garnets in the polymict xenoliths tend to be more enriched in Sr, Nb, and the LREE than the lighter-colored (Cr-poor) garnets (Fig. 6). Large variations exist in the HFSE Zr,

Hf, and Ti, particularly in the dark-colored garnets (Table 1 and Fig. 7). Even though the range in Zr and Ti concentrations in the pyropic garnets from the polymict xenoliths is within the field defined by P-type diamond inclusions and peridotitic garnets from worldwide localities (Fig. 7) [1,4,6,9,10,23,27–30], some garnets from JJG1414 are extremely enriched in Zr (> 200 ppm) but others have very low Zr (< 3 ppm) (Table 1 and Fig. 7). Thus it appears that the dark-colored (Cr-rich) garnets have relatively large variations of the REE, large ion lithophile elements (LILE), and HFSE, and more enrichment in the LREE and the LILE. Despite variations in Nb and Sr in relation to the degree of LREE enrichment, the Zr/Hf ratio remains nearly constant (Fig. 6).

With regard to Zr–Ti variation, the light-colored Cr-poor garnets have Zr and Ti concentrations that fall within the field of eclogite-type (E-type) diamond inclusions and eclogitic garnets from worldwide localities (Fig. 7). The dark-colored Cr-rich garnets have a broader range in Zr and Ti such that they plot beyond the confines of the field of the eclogitic and E-type diamond inclusion garnets. The E-type diamond inclusion and eclogite field overlaps with that of the P-type diamond inclusion and peridotitic paragenesis. This is consistent with the initial description of these polymict rocks by Lawless et al. [12] who claimed the presence of eclogitic fragments. However, this is to be contrasted with the 'lherzolite affinity' for most garnets on the basis of Cr–Ca (Fig. 4). In addition the garnets in the polymict rocks are similar to garnets from phlogopite-bearing, Fe-metasomatized and/or fertile peridotites [19]. This is consistent with the nature of the polymict rocks.

5. Oxygen isotope geochemistry

Oxygen isotopic compositions of pyropic garnets from the Kimberley polymict peridotites, South Africa, are listed in Table 1 and a histogram is plotted in Fig. 8 [17]. Overall garnets from polymict rocks show a similar oxygen isotope composition to those from P-type diamond
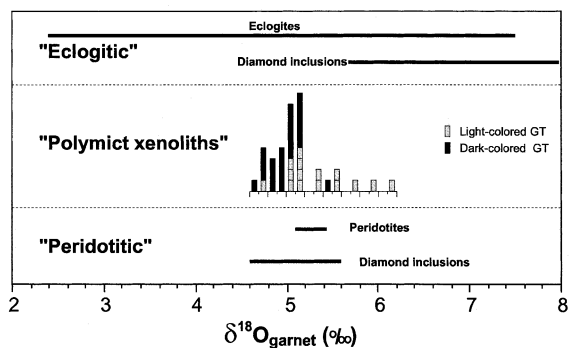
Fig. 8. Histogram of oxygen isotope compositions in garnets (after Zhang et al. [17]) from the Kimberley polymict xenoliths, South Africa, compared with the range of oxygen isotopes in garnets from P-type diamond inclusions and peridotites as well as E-type diamond inclusions and eclogites worldwide [3,8]. Note that the garnets from polymict xenoliths display a greater range in oxygen isotopes similar to P-type diamond inclusions and peridotites. Some garnets occur in the polymict peridotites with higher oxygen isotope ratios similar to that observed in eclogites and E-type inclusions.

inclusions and kimberlite-borne peridotite xenoliths from worldwide localities. This is consistent with conclusions based on the major element chemistry [12]. Relative to other peridotitic garnets, garnets from polymict xenoliths exhibit a larger $\delta^{18}O$ range (> 1.5‰) and the majority of analyses have a lower $\delta^{18}O$ ratio. This is particularly true for dark-colored (Cr-rich) garnets, the majority of which have lower $\delta^{18}O$ than the lower limit of peridotitic garnets. In contrast, light-colored (Cr-poor) garnets have higher $\delta^{18}O$ with a few samples extending to more than 6‰. The relatively restricted range in $\delta^{18}O$ values, and the lack of extreme $\delta^{18}O$ values, makes any similarity with E-type diamond inclusions or eclogites unlikely (Fig. 8).

Oxygen isotope variations in garnets from polymict xenoliths generally correlate with major (Fig. 9) and trace element data (Fig. 10) [17]. An increase in the oxygen isotope ratio of the garnets (relative to mantle values) is accompanied by a decrease in Cr, Ca and an increase in Fe although the latter is less systematic. A parallel change in the extent of LREE enrichment is observed and a decrease in Sr and Nb. The dark-colored (Cr-rich) garnets have lower oxygen iso-
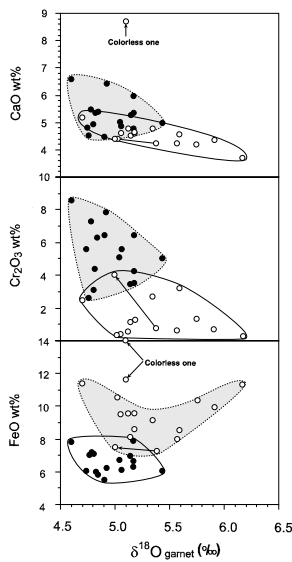
Fig. 9. Oxygen isotope correlation with major element abundances in garnets from the Kimberley polymict xenoliths. Note that the depletion of oxygen isotopes in garnets is accompanied by an increase in Cr, Ca and a decrease in Fe. If the depletion in oxygen isotopes is accomplished by melt migration those melts are enriched in Ca and Cr. Open circles and filled circles represent light-colored and dark-colored garnets, respectively.

tope ratios, a larger range (and more enrichment) in major and trace elements compared to the light-colored (Cr-poor) garnets (Figs. 9 and 10). In this respect the light-colored (Cr-poor) garnets are closer to a garnet precursor composition (i.e. LREE-depleted lherzolite; Fig. 5a).

6. Discussion

The data presented in this paper allow us to draw the following conclusions about the garnets in polymict xenoliths.
1. **Mantle peridotites**: Cr–Ca relationships in polymict garnets are similar to garnet-facies mantle peridotites. However, there is no similarity to low calcium harzburgites/dunites found in cratonic keels.
2. **Megacrysts**: Garnets in polymict peridotites have Cr contents similar to low Cr garnet megacrysts (75–200 km).

3. **Diamond inclusions**: On the basis of oxygen isotope ratios (ca. 1.5‰) garnets in polymict xenoliths are similar to garnets occurring as solid inclusions (P-type) in diamonds.
4. **Eclogite**: Garnets in polymict peridotites have Zr–Ti variation similar to that observed in solid inclusions (E-type) in diamond and garnets occurring in eclogites. However, this petrogenetic link is not supported by a restricted range in $\delta^{18}O$ values.

These observations indicate that the garnets in polymict peridotites have strong petrogenetic affinities with peridotites and weaker links to eclogite parageneses. In particular the similarities extend to the constituent minerals in garnet–diamond facies (>80 km) clinopyroxene-bearing peridotites like lherzolite. The presence of lherzolite contrasts with the predominance of clinopyroxene-free peridotites in kimberlite pipes, i.e. harzburgite and dunite [21]. Such a contradiction may be explained by harzburgites and dunites requiring the infiltration of silica-rich melts [13]. These melts have the potential of transforming lherzolite precursor to harzburgite by the dissolution of clinopyroxene and the preferential growth
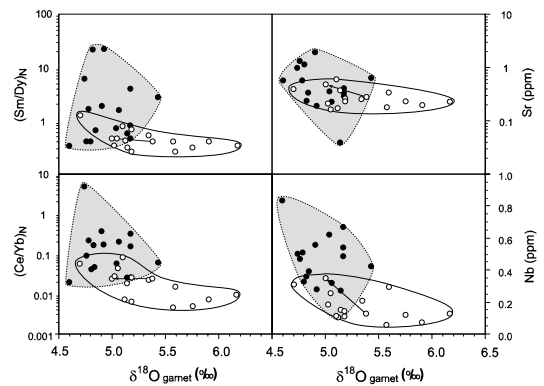

Fig. 10. Oxygen isotope correlation with trace element abundances in garnets from the Kimberley polymict xenoliths. The normalized Ce/Yb ratio represents an overall LREE enrichment in garnet. The normalized Sm/Dy ratio reflects the slope of the MREE segment in the REE profile. Note that a depletion in oxygen isotopes in garnets was accompanied by an enrichment in the LREE, Nb, Sr, and the MREE as well as Fe, Ca and Cr (Fig. 9). Open circles and filled circles represent light-colored and dark-colored garnets, respectively.

of orthopyroxene. It remains to be seen to what extent the minerals preserved in the polymict peridotites have retained mineral evidence of a widespread lherzolite precursor in the keel.

7. Elemental and oxygen isotopic disequilibrium: metasomatic effects

The large intra- and inter-mineral variability in elemental concentrations and oxygen isotopes may indicate that the garnets were affected by melt transfer processes inextricably linked to deformation processes (i.e. fluid-assisted). Melt-related or metasomatic effects are well illustrated by the correlation between major elements, trace elements, and oxygen isotopes in the garnets (Figs. 4, 6, 7, 9–11). The excellent positive correlation between the LREE and the LILE (Fig. 6) and the broadly negative correlations between oxygen isotope ratios and Cr, Ca (Fig. 9) and trace elements (i.e. LREE/HREE, Nb and Sr) (Fig. 10) indicate that the LREE enrichment in garnets was accompanied by an increase in Nb, Sr, Ca, and Cr and a depletion in ^{18}O. Enrichment in the LREE, Nb, Sr, Ca and Cr and modification of the O isotope ratio may have involved a melt similar to that involved in the formation of ilmenite–rutile–phlogopite–sulfide veins in mantle peridotites [36]. These melts were depleted in ^{18}O and had a constant Zr/Hf ratio (Figs. 6 and 7). However, for some reason the process did not attain full chemical equilibrium possibly because the entrainment process very effectively froze the processes in time, i.e. at the time of kimberlite emplacement.

Factors that will affect the degree to which the trace elements and oxygen isotopes re-equilibrate with a melt include: garnet composition, grain size, melt composition, pressure–temperature conditions [24,37–39]. The composition of the protolith garnet is difficult to determine but one can assume that those garnets with REE characteristics consistent with formation in a refractory protolith (i.e. low Ce/Yb ratio) are the closest to the precursor in composition. In this case these are the light LREE-depleted garnets which tend to be low in Cr and Ca. With regard to garnet grain

size it is reasonable to assume that small garnets in close proximity to intergranular small volume melts will more fully re-equilibrate than large grains. The existence of negative correlations between the grain size and the concentration of Cr, Ca, Nb, Sr, and the LREE (Fig. 3) indicates that garnets with smaller grain size have more fully equilibrated with the melt. This is particularly true for the dark-colored LREE-enriched garnets. Also, garnets with smaller grain sizes tend to have lower $\delta^{18}O$, a value closer to that of the 'melt'. In contrast, the light-colored garnets with a larger grain size have preserved some of the characteristics of the garnet precursor.

Another point that should be mentioned is that garnets in polymict rocks display a correlation between REE enrichment and Fe content that is similar to that observed in garnets in kimberlite-borne peridotites from South Africa (Fig. 11). Garnets with low FeO contents show a higher
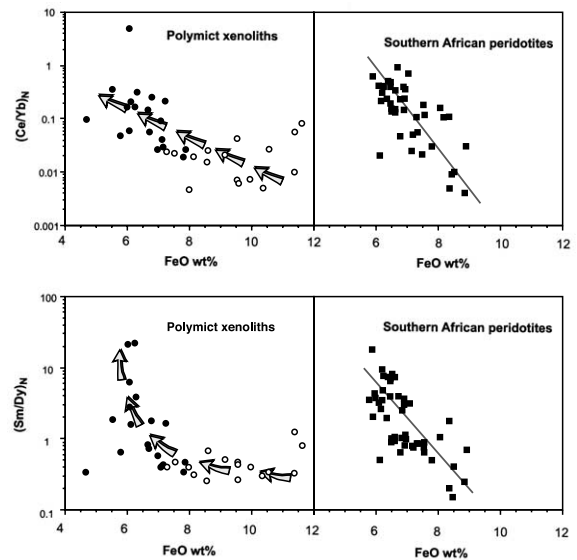

Fig. 11. REE compositions versus Fe content in garnets from polymict xenoliths, South Africa, compared with those from a variety of peridotites and mineral concentrates from southern Africa kimberlites. Garnets from the polymict xenoliths are from this study and data from southern Africa peridotites and kimberlite concentrates are taken from Hoal et al. [24], Stachel et al. [4], and references therein. Note that the polymict garnets have a greater range in iron than many kimberlite-borne peridotites from South Africa.

overall LREE enrichment ((Ce/Yb)$_N$, Fig. 11), a greater degree of sinuosity (i.e. (Sm/Dy)$_N$) in the REE pattern (Figs. 5 and 11) and lower oxygen isotopes (Fig. 9). Since high FeO would normally be associated with melts, one must deduce from this that the low Fe in the garnets resulted from the uptake of Fe by a co-existing mineral, possibly ilmenite. LREE–FeO covariance is exhibited by garnets from a variety of on- and off-craton peridotites, diamond inclusions and kimberlite mineral concentrates from Kaapvaal craton, southern Africa [24].

8. Theoretical modeling

Fig. 12 is a modification of an earlier model
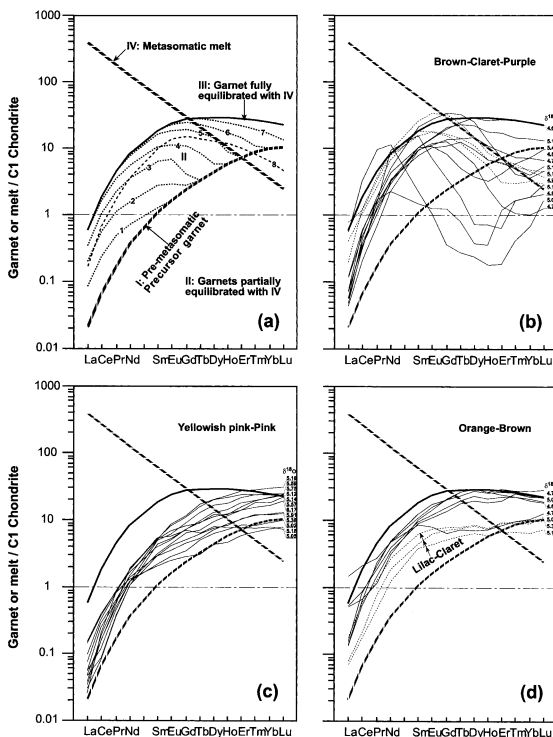
Fig. 12. Schematic illustration of the possible generation of LREE-enriched garnets by interaction of a refractory LREE-depleted garnet precursor with LREE-enriched melt. Theoretical REE profiles are compared with those measured in garnets from polymict xenoliths. C1 chondrite values are from Anders and Grevesse [22].

[24,40] and illustrates the REE composition of garnets produced by the reaction of a LREE-depleted garnet precursor and a LREE-enriched melt (detailed calculation procedures and the results are given in the Appendix). In the earlier application of this model [24,40] one partially equilibrated garnet was illustrated between the precursor and the fully equilibrated garnet. However, in Fig. 12 several transient garnet compositions are shown for comparison so that theoretically calculated REE profiles can be compared with measured REE patterns of the garnets from polymict xenoliths (Fig. 12b–d). In Fig. 12a, curve IV represents a LREE-enriched metasomatic melt based on group I and II kimberlites [24,41,42]. Curve I represents the pre-metasomatic garnet precursor. Curve III represents the theoretically calculated garnet from precursor I that was presumed to have fully equilibrated with the metasomatic melt IV. This is calculated using recently published garnet–silicate melt partition coefficients [43]. Curve II is a series of theoretical garnet compositions derived from precursor I presumed to have partially equilibrated with metasomatic melt IV. Since the garnet–silicate melt partition coefficient for the REE systematically increase from La to Lu and the estimated values for LREE (La–Nd), MREE (Sm–Dy), and HREE (Ho–Lu) fall within well-defined ranges ($\ll 0.1$, 0.1–2, and >2 respectively) [43,44], the LREE, MREE, and HREE may have behaved independently during metasomatic processes and may adjust, in a non-uniform way, to ambient changes induced by metasomatism or other mantle processes. The different order of magnitude of the partition coefficients for the REE in garnet may reflect the different rates at which the REE are able to react with the melt. Thus we postulate that the REE react with the infiltrating melt in a manner where $La > Ce > Nd > ... > Yb > Lu$. When kimberlitic melt (with the same REE composition as curve IV) infiltrates a mantle rock where a garnet is present (equiv. curve I), the compositional gradient between the garnet and the LREE-enriched melt will lead to a transient condition characterized by a sinusoidal REE pattern. A garnet with a partially equilibrated REE profile (i.e. curve II1) can be produced by partial

equilibrium with the melt, i.e. 7–15% equilibrium for La–Sm with no effect for all the other REE. When the reaction progresses to 10–35% equilibrium for La–Gd the other M–HREE remain unaffected and the newly formed garnet has a curve similar to II2. When all the LREE and the majority of the MREE are fully equilibrated with the melt a garnet with the composition of curve II7 crystallizes. Thus the progressive interaction of a refractory precursor with a kimberlitic melt produces partially equilibrated garnets. The peak in these partially equilibrated garnets is located at Sm to Gd corresponding to an increased degree of equilibrium. If the melt–garnet reaction is terminated by insufficient melt supply or rapid cooling (e.g. entrainment) the rock may preserve unequilibrated garnets. Furthermore, a partially equilibrated curve II8 is unique in that it needs all the REE to be partially affected by the melt to a certain degree.

In the polymict xenoliths (Fig. 12b–d) the pink garnets (Fig. 12c) have very similar REE profiles to that of the precursor with some garnets similar to the calculated curve II1 or II2. This suggests that these garnets were less affected by metasomatic processes thus preserving more information about the provenance of the precursor, consistent with textural evidence and oxygen isotope data. In the case of these garnets the oxygen isotopic composition is similar to that of average mantle [3,17]. The dark-colored garnets are more complicated (Fig. 12b,d) and display chondrite-normalized REE patterns that resemble curves II3–II5. The MREE enrichment and LREE depletion in these garnets relative to calculated REE profiles may indicate that the melt–matrix/metasomatic process was more complicated than implied by the model. Some dark-colored garnets (Fig. 12b,d) exhibit chondrite-normalized REE patterns like curves II6–II7 suggesting near total equilibrium with the melt. In others (Fig. 12d) the chondrite-normalized REE patterns are more akin to curve II2–II3 indicating that they have not fully equilibrated with the melt. It should be noted that the simple reaction model is insufficient to illustrate all the envisioned REE patterns for the garnets in the polymict xenoliths, especially for the dark-colored garnets. Other processes such as the diffusional re-equilibration with melt percolation, i.e. the chromatographic REE fractionation, must be involved in their genesis. Chromatographic effects [37] related to porous melt flow are believed to be a major reaction mechanism responsible for the inter-REE fractionation since there exists a significant variation of garnet solid/melt partitioning between LREE and HREE. This will enhance the diversity in REE patterns in garnets. In addition, the differences in precursor garnet compositions and the partition coefficients may also play a role in the discrepancies between the calculated and the measured patterns because we use the same parameters to do the calculation.

In Fig. 12b–d the LREE characteristics of the garnets in the polymict rocks are compared with theoretically modeled garnets produced by reacting protolith garnet with infiltrating kimberlite-like melt. It is clear that the somewhat simplistic modeling can explain the REE characteristics of some but not all of the garnets in the polymict rocks. In Fig. 12b, for example, the garnets have significant fluctuations in the REE profile that do not compare with Fig. 12a. The MREE enrichment and LREE depletion in these garnets relative to calculated REE profiles may indicate that the melt–matrix/metasomatic process was more complicated than implied by the model. Similarly in Fig. 12b garnets display chondrite-normalized REE patterns that resemble curves II3–II5 (Fig. 12a) indicating a disequilibrium situation while others have chondrite-normalized REE patterns like curves II6–II7 indicative of near total equilibrium with the melt. In Fig. 12c the chondrite-normalized REE patterns are more akin to curve II2–II3 indicating that they have not fully equilibrated with the melt. This suggests that these garnets were less affected by metasomatic processes thus preserving more information about the provenance of the precursor, consistent with textural evidence and oxygen isotopes. In the case of these garnets the isotopic composition is similar to that of average mantle [3,17].

Modeling indicates that the large trace element variations, together with the heterogeneities in major elements and oxygen isotopic ratios, of garnets in polymict xenoliths cannot be accounted for with one simple garnet precursor. This sug-

gests the existence of multiple garnet precursors, i.e. mixed provenance. The garnets were most likely modified by infiltrating metasomatic melts [11,24]. It appears that the dark-colored garnets were more affected by the metasomatic process than the light-colored garnets, in other words, light-colored garnets preserve more information about the nature of the garnet protolith/precursor. However, it is difficult to establish to what extent the mantle garnets were produced solely by melt–rock reaction. An additional process such as mantle deformation processes may have been responsible for juxtaposing minerals of distinct/polybaric provenance. Indeed, the inextricable link between deformation and melt movement would explain the concomitant modification of these minerals by melts.

Hypothetical melt compositions in equilibrium with those garnets that appear to have equilibrated with the melt can be calculated using garnet–melt partition coefficients [43]. The lack of a negative Ti and Zr anomaly and the general parallelism to kimberlites and lamproites indicates that these garnets were affected by K-rich melts (e.g. kimberlite or lamproite). The lower trace element concentration than the composition of Kaapvaal kimberlites may suggest that the melt was not the host kimberlites but more akin to a proto-kimberlite. However, the extreme enrichment in LREE and Nb in the rims of zoned garnets may reflect a different process. These melts are also similar to those calculated for fully equilibrated garnets from on-craton peridotites [24].

9. Conclusions

1. Peridotite/lherzolite paragenesis: Garnets found in polymict peridotites have chemical affinities with peridotite parageneses from cratonic keels, especially lherzolites (i.e. clinopyroxene-bearing).
2. Keel lithostratigraphy: Given the predominance of highly magnesian, clinopyroxene-free peridotites (i.e. garnet–diamond facies harzburgites and dunites) in the Kaapvaal cratonic keel, the 'lherzolite' parentage of the polymict

minerals is somewhat problematical and may relate to melt metasomatic processes.
3. Melt-assisted deformation: The mineralogy, elemental abundances and oxygen isotopic geochemistry of garnets in polymict peridotites from Kaapvaal, South Africa demonstrate that garnets have a complex origin more or less affected by melt-assisted deformation/crack propagation.
4. Preserved disequilibrium: Some garnets are in equilibrium with the melt but the majority remain unequilibrated. The preservation of elemental and isotopic disequilibria indicates that the entrainment process may have played a role in retaining such temporary features in time and space.
5. Paradox: Low Fe, high Cr–Ca garnets are LREE-enriched with low oxygen isotope ratios. High Fe, low Cr–Ca garnets are LREE-depleted with oxygen isotope ratios similar to the mantle average. This is counter-intuitive and points to unusual melt compositions and more significantly an unusual co-existing mineralogy (e.g. ilmenite, mica).

Appendix for Fig. 12

Calculation for the fully or partially equilibrated garnets from refractory precursor with the assumed metasomatic melt

	La	Ce	Pr	Nd	Sm	Eu	Gd	Tb	Dy	Ho	Er	Tm	Yb	Lu
Kd	0.0015	0.007	0.025	0.065	0.3	0.53	0.9	1.35	2	2.7	3.8	5	6.8	9
Refractory procurer I	0.005	0.04	0.015	0.17	0.16	0.09	0.45	0.12	1.06	0.33	1.16	0.21	1.6	0.25
Partially equilibrated II1	0.0203	0.1456	0.044	0.3218	0.189	0.09	0.45	0.12	1.06	0.33	1.16	0.21	1.6	0.25
	15%	13%	11%	9%	7%	N	N	N	N	N	N	N	N	N
Partially equilibrated II2	0.0473	0.336	0.1	0.715	0.405	0.1654	0.54	0.12	1.06	0.33	1.16	0.21	1.6	0.25
	25%	30%	25%	20%	15%	13%	10%	N	N	N	N	N	N	N
Partially equilibrated II3	0.081	0.616	0.2	1.6088	0.945	0.3816	0.81	0.12	1.06	0.33	1.16	0.21	1.6	0.25
	60%	55%	50%	45%	35%	30%	15%	N	N	N	N	N	N	N
Partially equilibrated II4	0.135	1.008	0.32	2.5025	1.62	0.636	2.16	0.3038	1.4	0.33	1.16	0.21	1.6	0.25
	100%	90%	80%	70%	60%	50%	40%	30%	20%	N	N	N	N	N
Partially equilibrated II5	0.135	1.12	0.4	3.575	2.43	1.0176	3.78	0.6075	3.5	0.486	1.16	0.21	1.6	0.25
	100%	100%	100%	100%	90%	80%	70%	60%	50%	30%	N	N	N	N
Partially equilibrated II6	0.135	1.12	0.4	3.575	2.7	1.272	4.86	0.81	4.9	0.972	2.28	0.26	1.6	0.25
	100%	100%	100%	100%	100%	100%	90%	80%	70%	60%	50%	40%	N	N
Partially equilibrated II7	0.135	1.12	0.4	3.575	2.7	1.272	5.4	0.9113	5.95	1.296	3.42	0.455	2.652	0.324
	100%	100%	100%	100%	100%	100%	100%	90%	85%	80%	75%	70%	65%	60%
Partially equilibrated II8	0.0405	0.42	0.16	1.6981	1.485	0.7632	2.97	0.5063	3.15	0.648	1.596	0.195	1.02	0.108
	30%	37.5%	40%	47.5%	55%	60%	55%	50%	45%	40%	35%	30%	25%	20%
Fully equilibrated III	0.135	1.12	0.4	3.575	2.7	1.272	5.4	1.0125	7	1.62	4.56	0.65	4.08	0.54
Metasomatic melt IV	90	160	16	55	9	2.4	6	0.75	3.5	0.6	1.2	0.13	0.6	0.06

Kd: Garnet partition coefficient relative to silicate melt (after Green [43] and references therein). I: Refractory garnet precursor assumed corresponding to the composition of 10% lower than the core of the pink garnet in Fig. 1B. II: Garnet partially equilibrated with metasomatic melt IV. Percentage shows the degree to which the equilibrium was reached and N represents no effect. III: Garnet fully equilibrated with metasomatic melt IV equals to Kd×IV, for example La III = 0.0015 × 90 = 0.135. IV: Assumed metasomatic melt obtained from the average composition of South African Group I and Group II kimberlites [39,41,42].

References

[1] W.L. Griffin, J.J. Gurney, C.G. Ryan, Variations in trapping temperatures and trace elements in peridotite-suite inclusions from African diamonds: evidence for two inclusion suites, and implications for lithosphere stratigraphy, Contrib. Mineral. Petrol. 110 (1992) 1–15.

[2] W.L. Griffin, S.Y. O'Reilly, C.G. Ryan, N.P. Pokhilenko, T.T. Win, E.S. Yefimova, Trace elements in garnets and chromites: diamond formation in the Siberian lithosphere, Lithos 29 (1993) 235–256.

[3] D.P. Mattey, D. Lowry, C.G. Macpherson, Oxygen isotope composition of mantle peridotite, Earth Planet. Sci. Lett. 128 (1994) 231–241.

[4] T. Stachel, K.S. Viljoen, G. Brey, J.W. Harris, Metasomatic processes in lherzolitic and harzburgitic domains of diamondiferous lithospheric mantle: REE in garnets from xenoliths and inclusions in diamonds, Earth Planet. Sci. Lett. 159 (1998) 1–12.

[5] N.V. Sobolev, G.A. Snyder, L.A. Taylor, R.A. Keller, E.S. Yefimova, V.N. Sobolev, N. Shimizu, Extreme chemical diversity in the mantle during eclogitic diamond formations: evidence from 35 garnet and 5 pyroxene inclusions in a single diamond, Int. Geol. Rev. 40 (1998) 567–578.

[6] W.L. Griffin, S.H. Shee, C.G. Ryan, T.T. Win, B.A. Wyatt, Harzburgite to lherzolite and back again: metasomatic processes in ultramafic xenoliths from the Wesselton kimberlite, Kimberley, South Africa, Contrib. Mineral. Petrol. 134 (1999) 252–260.

[7] W.L. Griffin, N.I. Fisher, J. Friedman, C.G. Ryan, S.Y. O'Reilly, Cr-pyrope garnets in the lithospheric mantle. I. Compositional systematics and relations to tectonic setting, J. Petrol. 40 (1999) 679–708.

[8] D. Lowry, D.P. Mattey, C.G. Macpherson, J.W. Harris, Oxygen isotope composition of syngenetic inclusions in diamond from Finsch Mine, RSA, Geochim. Cosmochim. Acta 63 (1999) 1825–1836.

[9] S.M. Glaser, S.F. Foley, D. Günther, Trace element compositions of minerals in garnet and spinel peridotite xenoliths from the Vitim volcanic field, Transbaikalia, eastern Siberia, Lithos 48 (1999) 263–285.

[10] W.Y. Wang, S. Sueno, E. Takahashi, H. Yurimoto, T. Gasparik, Enrichment processes at the base of the Archean lithospheric mantle: observations from trace element characteristics of pyropic garnet inclusions in diamonds, Contrib. Mineral. Petrol. 139 (2000) 720–733.

[11] S.R. Burgess, B. Harte, Tracing lithosphere evolution through the analysis of heterogeneous G9/G10 garnets in peridotite xenoliths, I: Major element chemistry, in: The J.B. Dawson volume, The VIIth Int. Kimb. Conf. Proc., 1999, pp. 66–80.

[12] P.J. Lawless, J.J. Gurney, J.B. Dawson, Polymict peridotites from the Bultfontein and De Beers mines, Kimberley, South Africa, in: The Mantle Sample: Inclusions in Kimberlites and Other Volcanics, IInd Int. Kimb. Conf. Proc., 1979, pp. 145–155.

[13] H.-F. Zhang, M.A. Menzies, J.J. Gurney, X.-H. Zhou,

Cratonic peridotites and silica-rich melts: diopside-enstatite relationships in polymict xenoliths, Kaapvaal, South Africa, Geochim. Cosmochim. Acta 65 (2001) 3365–3377.

[14] H.-F. Zhang, M.A. Menzies, D.P. Mattey, R.H. Hinton, J.J. Gurney, Petrology, mineralogy and geochemistry of oxide minerals in polymict xenoliths from the Bultfontein kimberlites, South Africa: implication for low bulk-rock oxygen isotopic ratios, Contrib. Mineral. Petrol. 141 (2001) 367–379.

[15] H.-F. Zhang, M.A. Menzies, X.-H. Zhou, F.-X. Lu, Textural and chemical zoning in garnets related to mantle metasomatism and deformation processes, Chin. Sci. Bull. 45 (2000) 174–180.

[16] B. Harte, M.B. Kirkley, Partitioning of trace elements between clinopyroxene and garnet: data from mantle eclogites, Chem. Geol. 136 (1997) 1–24.

[17] H.-F. Zhang, D.P. Mattey, N. Grassineau, D. Lowry, M. Brownless, J.J. Gurney, M.A. Menzies, Recent fluid processes in the Kaapvaal Craton, South Africa: coupled oxygen isotope and trace element disequilibrium in polymict peridotites, Earth Planet. Sci. Lett. 176 (2000) 57–72.

[18] F.R. Boyd, P.H. Nixon, Ultramafic nodules from the Kimberley pipes, South Africa, Geochim. Cosmochim. Acta 42 (1978) 1367–1382.

[19] W.L. Griffin, B.J. Doyle, C.G. Ryan, N.J. Pearson, S.Y. O'Reilly, R. Davies, K. Kivi, E. Van Achterbergh, L.M. Natapov, Layered mantle lithosphere in the Lac de Gras area, Slave Craton: Composition, structure and origin, J. Petrol. 40 (1999) 705–728.

[20] N.V. Sobolev, Y.G. Lavrentiev, G. Yu, N.P. Pokhilenko, L.V. Usova, Chrome-rich garnets from the kimberlites of Yakutia and their parageneses, Contrib. Mineral. Petrol. 40 (1973) 39–52.

[21] H.O.A. Meyer, Inclusions in diamond, in: P.H. Nixon (Ed.), Mantle Xenoliths, John Wiley and Sons, London, 1987, pp. 501–522.

[22] E. Anders, N. Grevesse, Abundances of the elements: meteoritic and solar, Geochim. Cosmochim. Acta 53 (1989) 197–214.

[23] N. Shimizu, N.V. Sobolev, Young peridotitic diamonds from the Mir kimberlite pipe, Nature 375 (1995) 394–397.

[24] K.E.O. Hoal, B.G. Hoal, A.J. Erlank, N. Shimizu, Metasomatism of the mantle lithosphere recorded by rare earth elements in garnets, Earth Planet. Sci. Lett. 126 (1994) 303–313.

[25] N. Shimizu, Rare earth elements in garnets and clinopyroxenes from garnet lherzolite nodules in kimberlites, Earth Planet. Sci. Lett. 25 (1975) 26–32.

[26] B.L. Beard, K.N. Fraracci, L.A. Taylor, G.A. Snyder, R.A. Clayton, T.K. Mayeda, N.V. Sobolev, Petrography and geochemistry of eclogites from the Mir kimberlite, Yakutia, Russia, Contrib. Mineral. Petrol. 125 (1996) 293–310.

[27] T. Stachel, G. Brey, J.W. Harris, Kankan diamonds I: from the lithosphere down to the transition zone, Contrib. Mineral. Petrol. 140 (2000) 1–15.

[28] N. Shimizu, C. Allègre, Geochemistry of transition elements in garnet lherzolite nodules in kimberlites, Contrib. Mineral. Petrol. 67 (1978) 41–50.

[29] N. Shimizu, S.H. Richardson, Trace element abundance patterns of garnet inclusions in peridotite-suite diamonds, Geochim. Cosmochim. Acta 51 (1987) 755–758.

[30] W.L. Griffin, D.R. Cousens, C.G. Ryan, S.H. Sie, G.F. Suter, Ni in chrome pyrope garnets: a new geothermometer, Contrib. Mineral. Petrol. 103 (1989) 199–202.

[31] W.L. Griffin, A.L. Jaques, S.H. Sie, C.G. Ryan, D.R. Cousens, G.F. Suter, Conditions of diamond growth: a proto microprobe study of inclusions in west Australian diamonds, Contrib. Mineral. Petrol. 99 (1988) 143–158.

[32] E.A. Jerde, L.A. Taylor, G. Crozaz, N.V. Sobolev, V.N. Sobolev, Diamondiferous eclogites from Yakutia, Siberia: evidence for a diversity of protoliths, Contrib. Mineral. Petrol. 114 (1993) 189–202.

[33] T.R. Ireland, R.L. Rudnick, Z. Spetsius, Trace elements in diamond inclusions from eclogites reveal link to Archaean granites, Earth Planet. Sci. Lett. 128 (1994) 199–213.

[34] L.A. Taylor, G.A. Snyder, G. Crozaz, V.N. Sobolev, E.S. Yefimova, N.V. Sobolev, Eclogitic inclusions in diamonds: Evidence of complex mantle processes over time, Earth Planet. Sci. Lett. 142 (1996) 535–551.

[35] G.A. Snyder, L.A. Taylor, G. Crozaz, A.N. Halliday, B.L. Beard, V.N. Sobolev, N.V. Sobolev, The Origins of Yakutian eclogite xenoliths, J. Petrol. 38 (1997) 85–113.

[36] H. Harte, P.A. Winterburn, J.J. Gurney, Metasomatic and enrichment phenomena in garnet peridotite facies mantle xenoliths from the Matsoku kimberlite pipe, Lesotho, in: M.A. Menzies, C.J. Hawkesworth (Eds.), Mantle Metasomatism, Academic Press Geology Series, London, 1987, pp. 145–220.

[37] J.L. Bodinier, G. Vasseur, J. Vernieres, C. Dupuy, J. Fabriès, Mechanisms of mantle metasomatism: geochemical evidence from the Lherz orogenic peridotite, J. Petrol. 31 (1990) 597–628.

[38] G. Vasseur, J. Verniers, J.L. Bodinier, Modelling of trace element transfer between mantle melt and heterogranular peridotite matrix, J. Petrol. Special Lherzolite Issue (1991) 41–54.

[39] E. Takazawa, F.A. Frey, N. Shimizu, M. Obata, J.L. Bodinier, Geochemical evidence for melt migration and reaction in the upper mantle, Nature 359 (1992) 55–58.

[40] N. Shimizu, Young geochemical features in cratonic peridotites from southern Africa and Siberia, A tribute to Francis R. (Joe) Boyd, in: Y. Fei, C.M. Bertka, B.O. Mysen (Eds.), Mantle Petrology: Field Observations and High Pressure Experimentation, Geochem. Soc. Spec. Publ. 6 (1999) 47–55.

[41] J.D. Kramers, C.B. Smith, N.P. Lock, R.S. Harmon, F.R. Bory, Can kimberlites be generated from an ordinary mantle?, Nature 291 (1981) 53–56.

[42] K.J. Fraser, C.J. Hawkesworth, A.J. Erlank, R.H. Mitchell, B.H. Scott-Smith, Sr, Nd and Pb isotope and minor

element geochemistry of lamproites and kimberlites, Earth Planet. Sci. Lett. 76 (1985) 57–70.

[43] T.H. Green, Experimental studies of trace-element partitioning applicable to igneous petrogenesis – Sodona 16 years later, Chem. Geol. 117 (1994) 1–36.

[44] N. Shimizu, I. Kushiro, The partitioning of rare earth elements between garnet and liquid at high pressures preliminary experiments, Geophys. Res. Lett. 3 (1975) 413–416.